Characterizing cement types in end-of-life concrete

A practical approach using handheld X-ray fluorescence

Alberda van Ekenstein, A.T.M.; Jonkers, H.M.; Ottelé, M.

DOI
10.1016/j.conbuildmat.2025.144293

Publication date
2025

Document Version
Final published version

Published in
Construction and Building Materials

Citation (APA)
Alberda van Ekenstein, A. T. M., Jonkers, H. M., & Ottelé, M. (2025). Characterizing cement types in end-of-life concrete: A practical approach using handheld X-ray fluorescence. *Construction and Building Materials*, *502*, Article 144293. https://doi.org/10.1016/j.conbuildmat.2025.144293

Construction and Building Materials 502 (2025) 144293

Contents lists available at ScienceDirect

Construction and Building Materials

journal homepage: www.elsevier.com/locate/conbuildmat

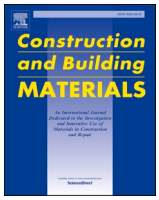

Characterizing cement types in end-of-life concrete: A practical approach using handheld X-ray fluorescence

A.T.M. Alberda van Ekenstein [a,b,*], H.M. Jonkers [a], M. Ottelé [a]

[a] Materials & Environment section, Dpt 3MD, Faculty of Civil Engineering and Geosciences, Delft University of Technology, Delft 2628 CN, the Netherlands
[b] Urban Mine B.V., Zaandam 1505 HS, the Netherlands

ARTICLE INFO

Keywords:
Circular concrete
Residual cementitious fines
Concrete recycling
Concrete harvesting
Handheld X-ray fluorescence
Cement identification

ABSTRACT

Reducing CO_2 emissions from concrete production requires effective recycling of cement, particularly its clinker component. Significant emission reductions depend on innovative techniques that extract high-quality cement fractions from recycled concrete, beginning with source separation strategies before demolition. This study developed a practical measurement approach using handheld X-ray fluorescence (HXRF) to identify cement types (i.e. cement classifications such as CEM I, CEM II/B-V, CEM III/B) in End-of-Life concrete. The research was conducted in two phases: First, laboratory testing of seven powder samples (milled river gravel and sand, three cement types: CEM I, CEM II/B-V and CEM III/B along with blast furnace slag and fly ash) and three cement paste prism types containing the three cement types established optimal measurement parameters and assessed moisture influence. Second, field measurements were taken on outdoor concrete blocks, containing the three cement types, after one year of weather exposure. Measurements were conducted on both the exposed surface and subsurface layers (after removing 0.1–5 mm of material). Results showed that powder samples can be accurately characterized with 10-second measurements, while concrete blocks require at least 20 s. HXRF measurements demonstrated good reproducibility with low coefficients of variation (CV) values, ensuring reliable cement type identification. Surface measurements are reliable only when the concrete is unaltered: coatings, paint, or weathering negatively affect accuracy, necessitating removal of the surface layer. Cement types were successfully distinguished using oxide concentrations (Al_2O_3, Fe_2O_3, P_2O_5, MgO) and their ratios (CEM III/B: $Al_2O_3/Fe_2O_3 > 9.0$, $MgO/Fe_2O_3 > 3.0$, $MgO/CaO > 0.11$, $Fe_2O_3/Al_2O_3 < 0.11$ and $Fe_2O_3/CaO < 0.04$; CEM II/B-V: $P_2O_5/CaO > 0.005$ and $P_2O_5/Fe_2O_3 > 0.1$; CEM I: $P_2O_5/CaO < 0.005$ and $P_2O_5/Fe_2O_3 < 0.1$). This study demonstrates that handheld XRF enables fast and reliable in-situ identification of the three studied cement types, supporting improved source separation and cement recycling strategies.

1. Introduction

Recycling of cement, particularly the clinker fraction, is critical for minimizing the environmental impact of concrete, as clinker production accounts for over 80 % of the CO_2 emissions associated with the cement production [2,26]. Current traditional crushing and recycling processes of End-of-Life concrete products only produce coarse (>4 mm) and fine (0 – 4 mm) aggregate fractions. While the coarse fraction is mostly used for lower grade applications, the fine fraction, which also includes cement, is not reused at all (Fig. 1) [1,7, 8]. To achieve significant reductions in CO_2 emissions, recycling processes should prioritize retrieving cement, which holds potential high-value reuse when separated effectively. Innovative crushing and recycling techniques are essential for this, as they enable the extraction of not only clean secondary aggregates, but more importantly the old cement in the form of residual cementitious fines (Fig. 2) [38].

Currently, recycled aggregates are often heterogenous in composition due to mixing various concrete waste streams from different sources, resulting in variations in quality, composition, and contaminations (Fig. 3) [29]. This heterogeneity limits the high-value reuse potential of particularly the fine fraction containing valuable cementitious components. To maximize the reuse potential, fine fraction separation strategies must be implemented to harvest the cementitious fraction. Such strategies should begin by characterizing End-of-Life (EoL) concrete,

* Corresponding author at: Materials & Environment section, Dpt 3MD, Faculty of Civil Engineering and Geosciences, Delft University of Technology, Delft 2628 CN, the Netherlands.
E-mail address: a.t.m.alberdavanekenstein@tudelft.nl (A.T.M. Alberda van Ekenstein).

https://doi.org/10.1016/j.conbuildmat.2025.144293
Received 6 August 2025; Received in revised form 4 October 2025; Accepted 29 October 2025
Available online 8 November 2025

particularly its cementitious components, before starting the demolition-, crushing- and recycling processes. This novel approach would enable upstream separation of concretes with specific cement types, thereby increasing the potential for high quality downstream separation and upcycling.

Separation at the source has thus the potential to reduce the heterogeneity of residual fines with respect to cementitious component types (e.g. clinker, ground granulated blast furnace slag (GGBFS), fly ash, etc.). From both environmental and financial perspectives, pre-separating Portland (clinker) cement-based concrete from concrete containing blended (lower clinker content) cement types is preferable, ensuring more homogeneous residual cementitious fine fractions. Moreover, specific applications may require particular cement types to optimize the new concrete mixture. Direct reuse or reuse after additional treatment of the residual cementitious fines lead to various material compositions: hydraulic cement, hydrated cement, pozzolanic material and filler [37,38]. The suitability for specific applications depends on the specific characteristics of the material and upcycling methods produce varying outcomes based on the material's origin. For instance, residual cementitious fines derived from Portland cement (CEM I) concrete are particularly suitable for CO_2 storage due to their higher portlandite and calcium oxide content compared to blended cements with lower clinker contents, such as blast furnace slag cements (BFS, CEM III) or fly ash cements (FA, CEM II). On the contrary, BFS containing fines appear more suitable for pozzolanic material formation and appear to carbonate faster than those consisting of FA [24,40].

The quantity of unreacted cement is another factor that determines the value of the fines from concrete crushing and recycling. Understanding the type, fineness and amount of cement in upstream concrete is therefore of interest. From an environmental perspective, concrete fines with high unreacted clinker content are preferred, as they can potentially replace primary clinker in new applications. Fines from blended cement-based concretes contain lower amounts of unreacted clinker, but may offer advantages in recovering unreacted BFS or FA particles for use in new concrete or geopolymer mixtures.

Optimizing the recycling process requires identifying the cement type in concrete prior to demolition. Handheld X-ray fluorescence (HXRF) represents a promising technique [1], as it determines the elemental composition of a material [5,14]. It is non-destructive, portable and enables rapid, on-site measurements [20,23]. The technique can distinguish cement types based on elemental or oxide composition, making it valuable to determine if potential differences allow differentiation in the type of cement in end-of-life (EoL) concrete, where cements may have been combined with other constituents.

While a limited number of studies have used HXRF for concrete and cement characterization [14,35], Nedelkjović et al. [28] specifically investigated HXRF for EoL concrete characterization and cement identification under controlled laboratory conditions. They concluded that HXRF has the potential to determine concrete quality at its origin, aiding in increasing reuse efficiency of recycled concrete components. However, their work was limited to laboratory settings, leaving gaps regarding practical field application feasibility under outdoor conditions. In practice, cement identification may be more challenging as environmental factors can alter the chemical composition of the concrete surface layers, e.g., through carbonation or erosion [3]. Additionally, coatings or paint layers can obscure the actual concrete composition, hindering accurate identification measurements. Environmental factors during HXRF surface measurements include moisture from rain and precipitation and efflorescence effects. Moisture causes deviations in measurement results by increasing the absorption of characteristic fluorescent X-rays, resulting in lower and potentially biased intensities [10,33]. The intensity decrease varies by elements, with heavier elements less affected than lighter elements [19]. Efflorescence, salt deposit formation on the concrete surface, occurs when calcium hydroxide (CH) migrates to the surface through diffusion or pore water evaporation [9,21, 41]. This leads to calcium carbonate formation on the concrete surface due to the reaction with atmospheric CO_2 [9,22,41], may hinder cement type determination in EoL concrete structures through HXRF surface analysis [21].

The present research therefore aims to develop a practical measurement approach using HXRF techniques to identify cement types in End-of-Life concrete under outdoor conditions. Unlike previous laboratory-based studies, this work provides field validation through several novel approaches: field validation under weathered conditions, surface layer removal analysis and oxide ratio analysis, resulting in a practical measurement approach. The experimental approach began with laboratory protocol development, focusing on measurement time and moisture influence on the accuracy of cement identification across

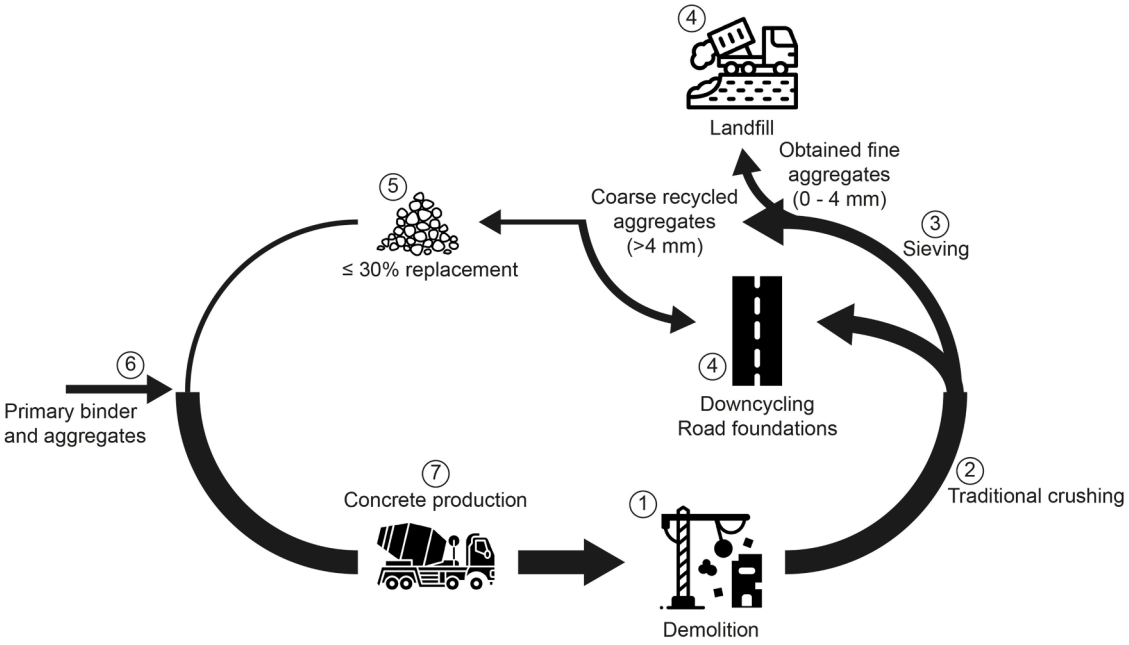

Fig. 1. Current traditional concrete recycling process adapted from [1]. Particularly the fine fraction (0 – 4 mm) of traditionally crushed concrete is landfilled, even though it contains the potentially most valuable cement fraction.

different cement types. This was followed by field testing of specially prepared concrete blocks that were aged at least one year under outdoor conditions. This testing validates its practical applicability when surface layers are eroded, contaminated, or affected by efflorescence, conditions often encountered in EoL concrete. Analyses were performed both before and after surface layer removal to evaluate whether cement types could be accurately identified.

2. Materials and methods

2.1. Handheld X-ray fluorescence

In this research, three categories of samples were prepared and characterized using HXRF: powders, cement paste prisms, and concrete blocks. The powders were analysed to investigate variations in the chemical composition of the primary materials found in concrete, which can aid in cement type identification, and to assess the impact of measurement time on the reliability of the results. Cement paste prisms were prepared in a laboratory setting to assess the influence of moisture on the measurement results and to determine whether a potential bias, relative to the actual chemical composition, needs to be considered as a result. In contrast to the controlled nature of the fine powders, the final category, concrete blocks, represents complex, heterogeneous outdoor samples, which are examined to assess the practical feasibility of the HXRF for concrete in outdoor conditions. Both measurement time and chemical composition were analysed to develop a method suitable for practical applications. In this study, a X-MET8000 Expert GEO HXRF device was used for this purpose. It features a 25 mm^2 high resolution silicon-drift detector and a Rh target X-ray tube, with robust fundamental parameters providing an analytical range from Mg to U. The measurement spot size is 10.7 × 9.4 mm, but can be reduced to a spot size with a diameter of 3 mm for increased resolution using a small-spot collimator. The instrument was calibrated using certified reference materials. Detection limits were evaluated using the instrument limit of detection (IDL), defined as the concentration required for an element to produce an X-ray signal greater than three times the standard deviation of the background noise level, and the method limit of detection (MDL), defined as the minimum concentration that can be measured and reported with 99 % confidence that the element's concentration is greater than zero [13]. Although handheld XRF instruments may exhibit precision and accuracy limitations compared to laboratory-based methods, the strong correlations observed between handheld and desktop measurements ($R^2 > 0.90$) indicate adequate analytical consistency for field-based measurements. Insight in the correlation between HXRF and desktop XRF are provided in Appendix B.

2.2. Powders

The primary powders analysed by HXRF in this research represent a set of the most commonly used mineral components in concrete, which can be classified into two main groups: aggregates and cements. For this study, the aggregates used are river gravel and river sand, which were milled to powders (<125 μm) in a Retsch mortar grinder RM200. The cement types chosen reflect the most commonly used ones in the Netherlands: Portland cement (CEM I), blast furnace cement (CEM III/B) and fly ash cement (CEM II/B-V). Since CEM III/B and CEM II/B-V are blends of CEM I with blast furnace slag and fly ash, respectively, these supplementary materials are also included among the powders examined in this study. A complete overview of the seven primary powders analysed in this study is provided in Table 1.

2.2.1. Measurement time

For the measurements the prepared powders were placed in sample cups and retained in these cups with a special thin film (Mylar® thin film: 3.6μm). These cups were then placed in a benchtop setup to which the HXRF was attached. The HXRF guide recommends a measurement time of 30 s to 5 min for powders to ensure reliable results, accounting for their heterogeneous nature [12]. However, shorter measurement times are preferred in practical applications if they can provide comparable accuracy. To assess the influence of measurement time, various durations were tested, namely 5, 10, 20, 30, 60, 90, 120, and 300 s. Reliability was calculated by using the 300-second measurement as the reference standard (100 % reliability) for each oxide. For shorter measurement durations, reliability was determined by comparing the measured oxide concentrations to their corresponding 300-second values and calculating the percentage deviation. A measurement

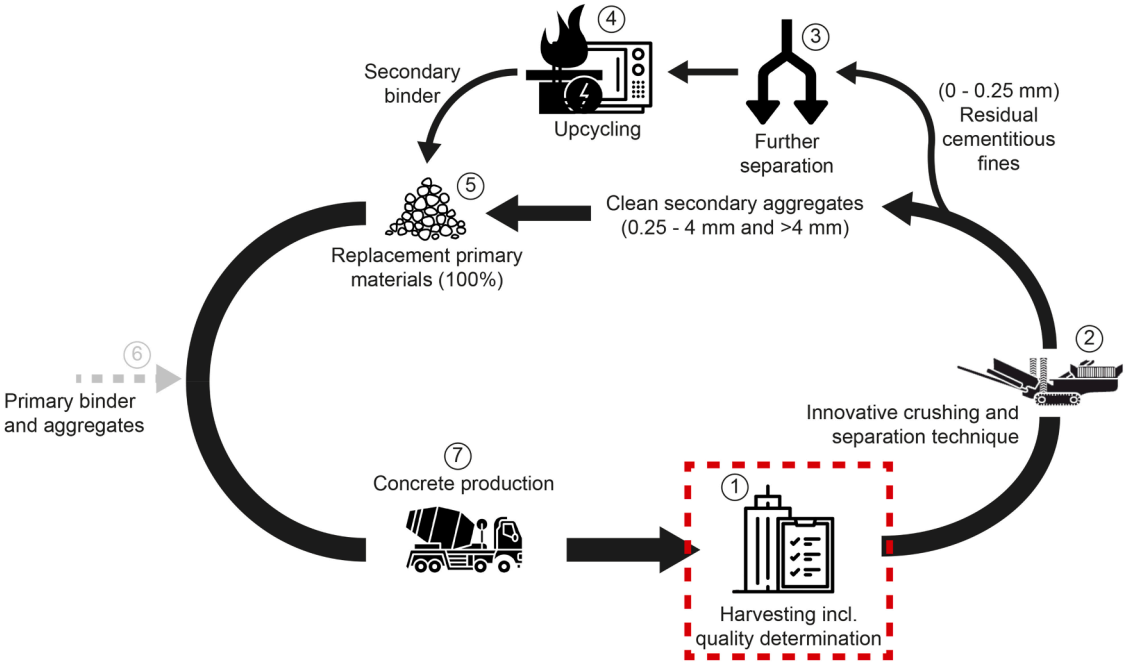

Fig. 2. Envisioned innovative concrete recycling process adapted from [1]. In this innovative recycling process both the fine and coarse aggregate fractions are fully reused as well as the cement is retrieved and reused.

duration was considered acceptable if it achieved at least 95 % reliability, meaning the oxide concentrations deviated by no more than 5 % from the 300-second reference values. To assess measurement reproducibility, triplicate analyses were performed on all measurement locations, both on the surface and after surface removal (Appendix A).

2.3. Cement paste prisms

Cement pastes were made of the three chosen cement types and hydrated in prism moulds (3 prisms per cement type) with a water-to-cement ratio of 0.5 and covered with a thin plastic sheet prior to demoulding to prevent evaporation of water. Mixing of the cement pastes was done in accordance with EN 196–1 [30]. After a day the prisms were removed from the moulds and stored in zip lock bags for at least 28 days at 20 °C until further testing. These cement prisms were used to study the impact of moisture on HXRF characterization. Apparent differences in detected chemical composition due to moisture is also expected to be relevant for concrete in practice. After the storage period (28 days in zip lock bags), the prisms were divided into three different groups to examine the possible influence of moisture variation on the HXRF analysis. Measurements (average of 6) were conducted on cement paste prisms in the laboratory setup subjected to the following conditions:

- Directly after storage in zip lock bags (fully hydrated) at room temperature (20 °C).
- Furnace dried at 105 °C until no further weight decrease (fully dried).
- Saturated in water for 1, 5 and 30 min (increasing level of water saturation).

2.4. Concrete blocks

Concrete blocks with three different known mixture designs and constituents were manufactured by Urban Mine B.V. to represent outdoor concrete structures. The primary difference between the prepared concrete blocks was the type of cements used. These were chosen to represent the most commonly used cement types in the Netherlands. Five blocks, each measuring 160 × 80 x 80 centimetres were produced for each cement type. These blocks were stored outdoors for one year (2022–2023) before HXRF measurements were conducted. During this period, climatic conditions recorded by the Royal Netherlands Meteorological Institute included 14 tropical days (maximum temperature ≥30°C), 71 frost days (minimum temperature <0°C), and substantial precipitation (1789 mm) typical of the Dutch maritime climate [16,17]. Table 2 provides an overview of the mixture design for the concrete blocks.

Table 1
Overview of the composition of the studied primary powders.

Powders	River gravel (milled)	River sand (milled)	CEM I	Blast furnace slag	Fly ash
River gravel	100 %	-	-	-	-
River sand	-	100 %	-	-	-
CEM I	-	-	100 %	-	-
CEM II/B-V	-	-	70 %	-	30 %
CEM III/B	-	-	30 %	70 %	-
Blast furnace slag	-	-	-	100 %	-
Fly ash	-	-	-	-	100 %

2.4.1. Measurement setup

The concrete blocks were stacked outdoors to serve as a storage bay. To ensure that HXRF measurements were consistently taken at the same spot on the concrete blocks, a suspending standard was developed (Fig. 4). The standard was positioned over the highest block so that a rail hung down on one side. Depending on the height of the stacked blocks, the rail was supported either from the ground or by an anchor attached to the rail via an elastic rope. This standard enabled vertical movement of the HXRF measurement equipment, ensuring that multiple measurements could be taken at the exact same spot along the height of the blocks. Furthermore, the measurement device could be positioned on either side of the rail due to the rotatable holder.

2.4.2. Efflorescence effect and measurement time

Layers with high calcium content on the concrete surface (e.g. due to carbonation of aged concrete or the efflorescence effect) may hinder accurate identification of the used cement type of the underlying concrete. To determine whether such a carbonation or alternatively efflorescence effect occurring on the produced concrete blocks complicates the cement identification process, a specific set of measurements was performed. Therefore, the surface of each block was divided into six measurement locations (Fig. 5). Measurements were subsequently conducted both on the untreated concrete surface and after removing the top surface layer using an angle grinder with a flap disc to a depth between 0.1 – 5 mm to minimize the influence of carbonation, efflorescence or potential environmental contamination effects.

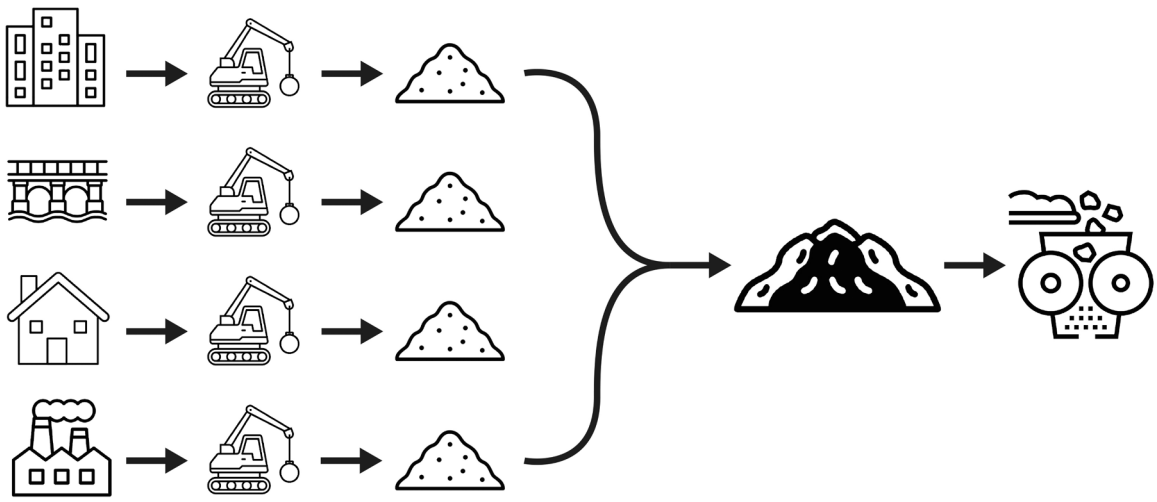

Fig. 3. Possible concrete sources of various qualities, compositions and contamination resulting in heterogeneous quality concrete waste streams. These waste streams are currently often pooled and mixed at the recycling plant prior to recycling what limits the high-quality recycling potential of particularly the fine fraction.

Table 2
Mixture designs (values in kg per m^3 concrete) with varying cement types for the concrete blocks analysed in this study.

	Mixture design [kg]							
	River gravel 4/32	River sand 0/4	CEM I 52.5 R	Blast furnace slag	Fly ash	Super plasticizer	Water	Total
Block 1: CEM I	1010	860	330	0	0	2	162	2364
Block 2: CEM III/B	1010	860	100	230	0	2	162	2364
Block 3: CEM II/B-V	1010	830	230	0	100	2	162	2334

Fig. 4. Suspended standard for in situ HXRF measurements of concrete blocks.

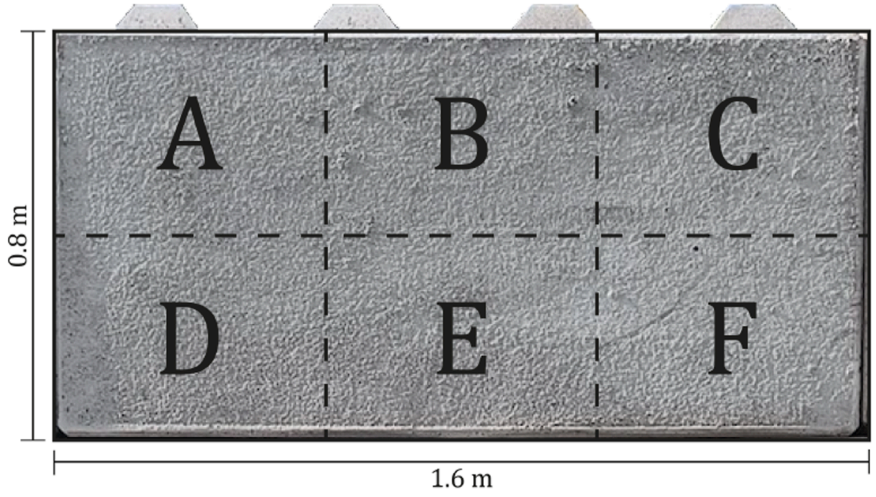

Fig. 5. Division of concrete block surface into six measurement locations.

XRF measurements can be affected by factors such as grain size, heterogeneity, and mineralogical composition. To mitigate these effects, the preparation of pressed pellets or fused beads containing the sample of interest is often recommended [15]. However, this approach is not feasible for field measurements. Consequently, measurement times were not only evaluated for the powders, but also the concrete blocks. The same measurement times evaluated for the powders were applied for the concrete blocks. The six measurement locations mentioned, were also used to assess how the measurement time affects the reliability of the concrete block results.

3. Results

3.1. Powders

3.1.1. Measurement time of powders

In total, 7 different powders (as listed in Table 1) and the effect of 8 measurement times (5, 10, 20, 30, 60, 90, 120, 300 sec) were analysed. The aim was to determine the minimum HXRF measurement time required to achieve reliable oxide identification in various cementitious powders, while maximizing testing efficiency for industrial applications. By identifying the optimal minimum measurement times for different powder types, more efficient quality control procedures without

compromising accuracy can be achieved. A theoretical reliability threshold of 95 % [25,27,31] was used as the initial benchmark for acceptable oxide identification. However, lower reliability thresholds are acceptable when oxide composition variations remain distinctive for cement identification.

Fig. 6 provides an overview of the change in reliability for the increasing measurement times used for all the powders. All investigated powders show a reliability of oxide identification above the 95 % threshold when using measurement times of 50 s or longer. CEM I appears most sensitive to measurement time, as all other powders reached the 95 % reliability threshold with just 30 s of measurement time and stayed above 90 % reliability for shorter measurement times.

In practice, further reduction in measurement time may be feasible depending on the required level of accuracy. Supplementary Table S1 illustrates the impact of measurement time on the composition of CEM I powder. For most specific oxides, lowering the 95 % reliability threshold and shortening the measurement time still yield comparable compositions. However, the largest deviations are observed for MgO across all powders. For FA and CEM II/B-V, this effect is particularly pronounced at shorter measurement times (5, 10, and 20 s) where it is the only oxide below 95 % reliability. Similarly, CEM I exhibits this reduced reliability pattern, with an additional significant reliability decrease observed at the 60-second measurement interval. Notably, the reliability of MgO is particularly low at 5 s, but increases to more than twice that value by the 10-second mark. This deviation in MgO reliability appears to be smaller for materials with larger amounts of MgO present in their chemical composition, such as BFS and CEM III/B. For these materials, the lowest reliability is 80.8 % at 5 s and 76.1 % at 20 s, respectively. Additionally, P_2O_5 shows slight variations in its reliability, with the smallest reliability being 93.8 % for CEM III/B at 60 s and 89.6 % for BFS at 5 s. Fe_2O_3 remains above a 95 % reliability threshold, except for the 5-second measurement in BFS (94.5 %).

3.1.2. Chemical composition of cement types

Table 3 shows the oxide composition percentages of the three cement types as an example from literature [4,11,34,36] and obtained through HXRF measurements in this study. To distinguish CEM I from CEM III/B and CEM II/B-V, the CaO and SiO_2 content could potentially provide a first indication. However, typically applied siliceous aggregates also contain large amounts of SiO_2, which might interfere with the cement type specific Ca/SiO_2 ratios. More specific elements might therefore be required for proper cement type identification. The amount of Al_2O_3 is significantly lower in CEM I compared to the other two cement types, because the latter contain supplementary cementitious materials (slag and fly ash, respectively) that are naturally rich in Al_2O_3. To differentiate between CEM II/B-V and CEM III/B, P_2O_5, Fe_2O_3 and MgO contents are of interest as they reflect the different SCM compositions: MgO content is higher in CEM III/B due to the magnesium-rich nature of blast furnace slag, while Fe_2O_3 levels are higher in CEM II/B-V due to the iron content typically found in fly ash. P_2O_5 provides additional discrimination between these slag- and fly ash-containing cements.

3.2. Cement paste prisms – effect of moisture

In outdoor applications, moisture conditions can vary considerably across different concrete elements and locations. This variation in moisture content can impact the accuracy of HXRF measurements and result in apparent differences in the detected chemical composition. Fig. 7 illustrates the influence of various moisture incubation conditions on the apparent chemical composition of three cement types. Similar trends are observed across the different cement prisms. After drying the prisms in a furnace, a slight increase in SiO_2 and Al_2O_3 content and a decrease in CaO content was observed for the CEM III/B and CEM II/B-V prisms. The CEM I prisms showed an opposite trend. After saturation, the CaO content increased, while the SiO_2 and Al_2O_3 content decreased. No clear deviations were observed for the other oxides.

To differentiate deviations in chemical composition caused by moisture from those due to surface carbonation or the efflorescence effect, cement prisms were immersed in a water bath for varying durations, as described in Section 2.3. Table 4 presents the measurement results for three different cement types, recorded both before and after immersion for various residence times. The residence times tested were 1 min, 5 min, and 30 min. Measurements taken prior to immersion serve as the 0-minute baseline and are compared with the results obtained after the specified residence times.

The table indicates slight apparent changes in the chemical composition of the prisms for each residence time, especially after saturating for 30 min. An increase in the CaO content is observed as the residence time increases for CEM I prisms, whereas for the CEM III/B and CEM II/B-V prisms this is only observed after the 30 min saturation. The concentration of the other oxides generally decreases, except for Fe_2O_3 in all prisms, K_2O in CEM III/B and MgO in all prisms, which remain relatively consistent across all moisture conditions.

When considering the 1- and 5-minute residence times, the differences in chemical composition are comparable to the reference (0 min) measurements. For CEM I, a slight increase in CaO is observed, whereas

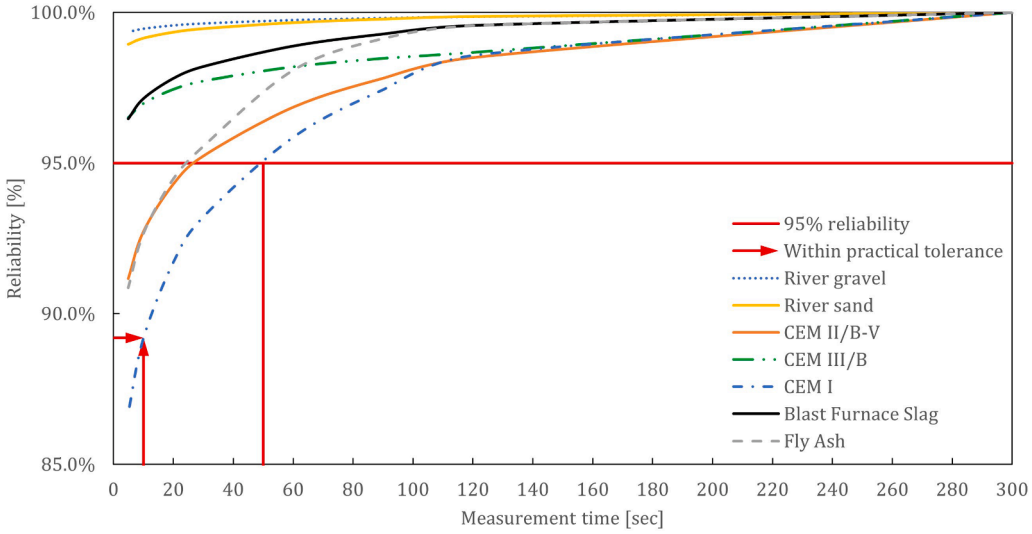

Fig. 6. Reliability of powder composition identification for different measurement times of the HXRF device. Achieving a 95 % reliability threshold requires 50 s of measurement time, but acceptable results for practical applications can be obtained with 10 s.

Table 3
Oxide composition percentages measured by HXRF and example oxide composition percentages from literature [4,11,34,36] as determined by XRF of the three cement types. Distinct differences between the cement types are observed.

		CaO	SiO_2	Al_2O_3	Fe_2O_3	MgO	Na_2O	K_2O	TiO_2	P_2O_5	SO_3	Ref.
CEM I	Lit.	60–67	17–25	3 – 8	0.5 – 6.0	0.1 – 5.5	0 – 0.8	0 – 1.7	0.1 – 0.4	0.1 – 0.2	1 – 3	[11, 34]
	HXRF	64.64	22.33	5.29	2.02	1.49	n.d.	1.15	0.22	0.29	6.97	-
CEM III/B	Lit.	48.20	30.1	10.10	1.00	6.80	0.3	0.3	-	-	2.5	[36]
	HXRF	50.06	29.95	9.39	0.78	4.61	n.d.	0.93	0.84	0.37	4.12	-
CEM II/B-V	Lit.	40.79	28.44	14.11	2.93	2.93	0.55	1.44	0.45	0.45	4.33	[4]
	HXRF	46.15	30.8	9.92	3.72	0.7	n.d.	1.59	0.52	0.56	5.49	-

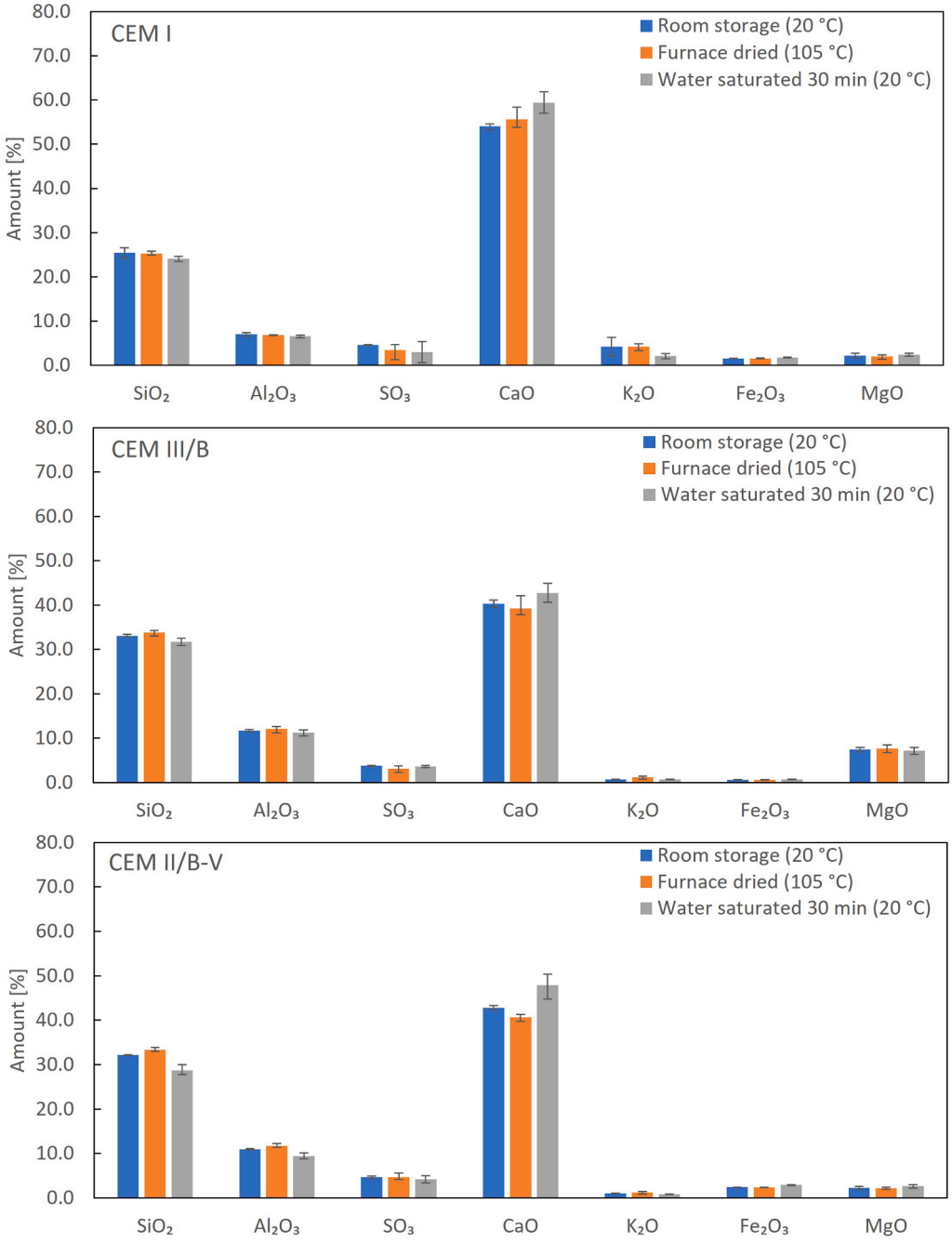

Fig. 7. Influence of moisture on the chemical composition of hydrated cementitious prisms. The largest change in concentration was observed for SiO_2 and CaO, but they remained within the cement identification range.

Table 4
Influence of the saturation time on the apparent chemical composition of hydrated cementitious prisms. Changes to the measured concentrations remained within the range for cement identification.

		SiO_2	Al_2O_3	SO_3	CaO	K_2O	Fe_2O_3	MgO
CEM I	0 min	25.4	7.0	4.6	54.0	4.2	1.6	2.2
	1 min	25.5	7.0	2.8	57.0	2.5	1.7	2.6
	5 min	25.0	6.8	2.4	58.4	2.3	1.7	2.4
	30 min	24.1	6.5	3.0	59.4	2.1	1.8	2.4
CEM III/B	0 min	33.1	11.8	3.8	40.3	0.7	0.6	7.5
	1 min	33.1	11.8	3.8	40.2	0.7	0.6	7.4
	5 min	33.0	11.8	3.7	40.4	0.7	0.6	7.6
	30 min	31.7	11.3	3.6	42.8	0.7	0.7	7.2
CEM II/B-V	0 min	32.1	10.9	4.7	42.8	1.0	2.4	2.3
	1 min	31.5	10.6	4.7	43.8	1.0	2.6	2.1
	5 min	32.3	11.1	5.2	41.6	0.9	2.5	2.6
	30 min	28.7	9.4	4.2	47.9	0.9	2.9	2.7

CEM III/B and CEM II/B-V show only minor deviations. Similarly, only small differences are observed for the other oxides. The only exceptions are K_2O and SO_3 in CEM I, which decreased after 1 min of saturation. However, for a residence time of 30 min, larger changes occurred.

3.3. Concrete blocks

3.3.1. Measurement time

Fig. 8 provides an overview of the change in reliability for different measurement times for the five concrete blocks and their three compositions. Similarly to the powders, the aim was to determine the minimum required measurement time to obtain reliable oxide results. However, the blocks potentially require different minimum measurement times due to their different physical properties and heterogeneity. Expectations are therefore that the minimum measurement time to obtain the same theoretical reliability threshold of 95 % increases for the concrete blocks. However, lower reliability is again acceptable when oxide composition variations remain distinctive for cement identification. By taking this into account, the approach is optimized for different sample types while maintaining reliable results. The investigated blocks demonstrate a reliability of oxide identification above the 95 % threshold when using measurement times of 80 s and longer, except for block 3.5 which crossed the 95 % threshold only at 190 s. For shorter measurement times the reliability remained above 85 %, except for blocks 2.5 and 3.5, which required measurement times of at least 20 s to achieve this reliability.

Fig.entary Figures S1-S3 and Supplementary Tables S2-S4 present an overview of the deviation in composition of the individual concrete blocks for different measurement times. The results indicate no significant variations in composition for measurement times ranging from 20 to 300 s. Similar to the powders, magnesium shows the largest deviations. Below 20 s, larger changes in composition were observed.

3.3.2. Surface layer composition of the concrete blocks

Concrete elements can generally be divided into three main layers as a result of the wall effect: a cementitious surface layer (about 0.1 mm), an underlying mortar layer (about 5 mm) and the bulk concrete layer [18,32]. The top layer characterized by HXRF should therefore particularly yield the chemical composition of the cement type used in the concrete. This approach aligns with the methodology developed in a laboratory setting by Nedelkjović et al. [28], which uses the cementitious surface layer to identify the cement type in concrete elements.

In this study, a total of six locations were measured on each block, resulting in 30 measurement locations for each cement type. Each location was measured three times and the averages of these measurements are presented in Fig. 9. To identify the tracer elements relevant for cement identification, the cement types were analysed using HXRF prior to being incorporated into the concrete mixture. The chemical composition of these cements is provided in Supplementary Table S5. These results reveal distinct deviations in all measured oxide concentration, particularly CaO, Al_2O_3, Fe_2O_3, MgO and P_2O_5. The Al_2O_3 concentration is relatively higher for CEM III/B and CEM II/B-V compared to CEM I. Furthermore, the CaO concentration is highest for CEM I, the MgO concentration for CEM III/B and the Fe_2O_3 and P_2O_5 concentrations for CEM II/B-V. This pattern is also observed in the average results of the surface layer measurements of the three corresponding concrete blocks, although the differences between the oxides are more nuanced. In particular, the range of CaO and MgO concentrations appears to fluctuate.

3.3.3. Removal of the surface layer

To eliminate the efflorescence effect and other potential influences on the outer layer, the surface of the concrete was removed to a depth between 0.1 – 5 mm. The same approach used for surface measurements was then applied. During the measurements, the HXRF was positioned between the aggregate particles as much as possible. The average results are shown in Fig. 10. Block 2 and 3 show an increased Al_2O_3 concentration compared to block 1. To distinguish between blocks 2 and 3, the oxide concentrations of MgO, Fe_2O_3 and P_2O_5 can be used. Higher oxide concentrations of MgO were observed for block 2, whereas block 3 showed higher concentrations of Fe_2O_3 and P_2O_5.

In addition to the oxide concentrations, the normalized ratios between certain specific oxides may also be of interest for identifying the cement type. Fig. 11 displays the normalized oxide ratios of interest for identifying the cement type in the concrete blocks. Ratios involving SiO_2 were not considered, because the studied concrete blocks contained siliceous aggregates. Block 2, containing CEM III/B cement, has various distinct ratio ranges that can be used for identification. It shows high ratios for Al_2O_3/Fe_2O_3 (>9.0), MgO/Fe_2O_3 (>3.0) and MgO/CaO (>0.11), whereas Fe_2O_3/Al_2O_3 (<0.11) and Fe_2O_3/CaO (<0.04) are significantly lower compared to the other blocks. Subsequently, blocks 1 (CEM I) and 3 (CEM II/B-V) differ based on their P_2O_5/CaO and P_2O_5/Fe_2O_3 ratios, which are both higher for block 3 (>0.005 and >0.1 respectively). Additionally, the Al_2O_3/CaO is generally lower for block 1, although this difference is less distinct compared to other ratios. The ranges for the various ratios are shown in Table 5.

4. Discussion

Establishing an optimal HXRF measurement approach is crucial for characterizing End-of-Life concrete both before and during the recycling process. This characterization represents a critical step for efficient recycling and successful upcycling of residual cementitious fines. In this context, upcycling refers to the transformation of these fines into high-quality secondary cements, which plays a vital role in reducing concrete-related CO_2 emissions by decreasing or potentially eliminating the need for primary cement production. Optimizing the HXRF measurement approach not only enhances field execution efficiency, but also improves the recognizability of the concrete composition. Reliable characterization ensures the production of high-quality residual cementitious fines suitable for high-value applications rather than being downcycled into lower-grade uses (Fig. 12). To advance this optimization, this study specifically examined the measurement time, moisture influence, and the impact of efflorescence on cement type identification.

4.1. Measurement time

From a theoretical perspective, the 95 % measurement reliability threshold [25,27,31] was considered when determining minimum measurement times. Results from the present study indicate that a minimum measurement duration of 50 s for powders and 80 s for concrete blocks is required to achieve the 95 % reliability standard. However, when the reliability threshold is decreased to 85 %, a value generally considered sufficient for accurate characterization and identification, measurement times can be reduced to 10 s and 20 s,

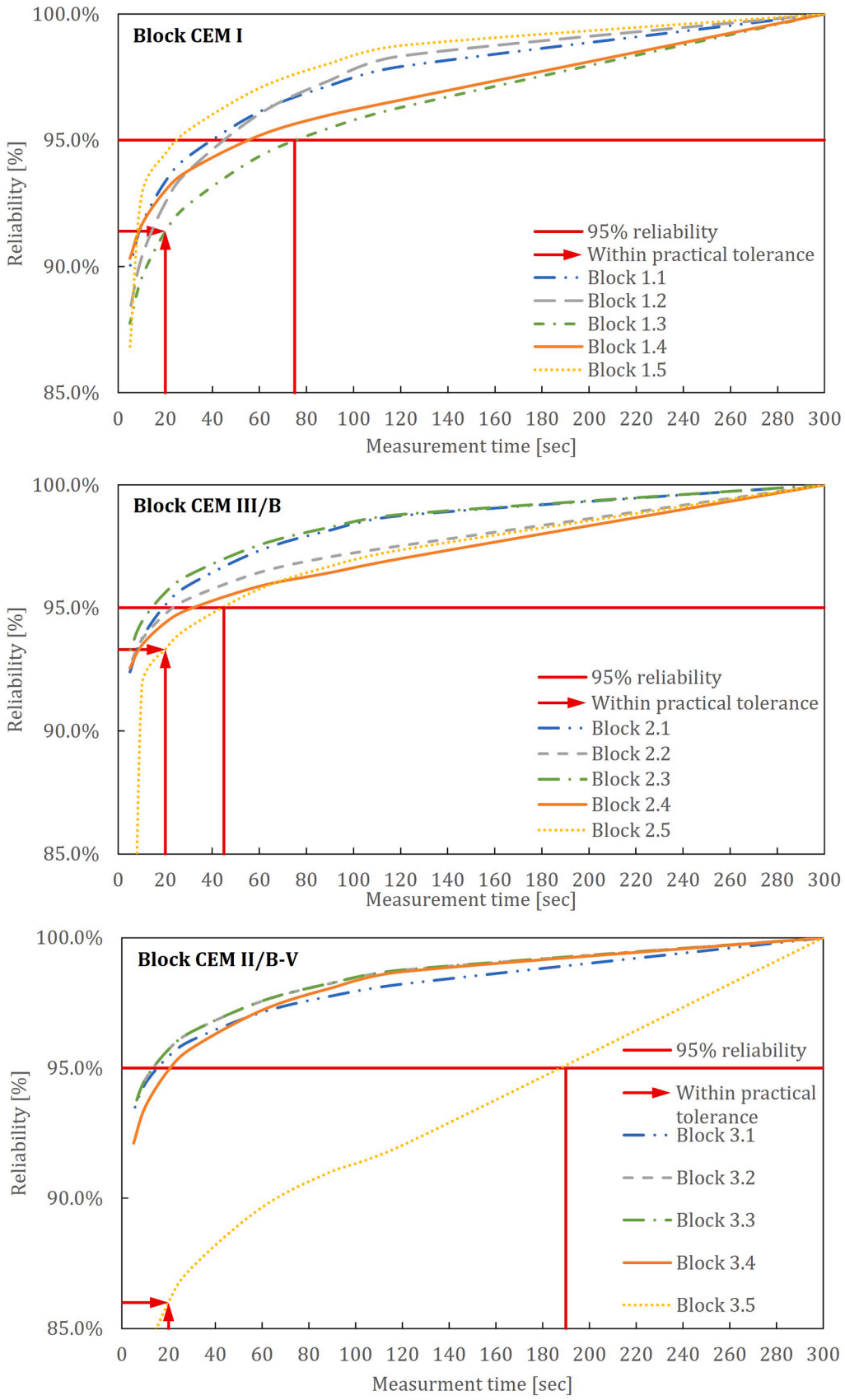

Fig. 8. Reliability of the concrete block composition for different measurement times of the HXRF. Achieving a 95 % reliability threshold requires 80 s of measurement time in most cases, but acceptable results for practical applications can be obtained with 20 s.

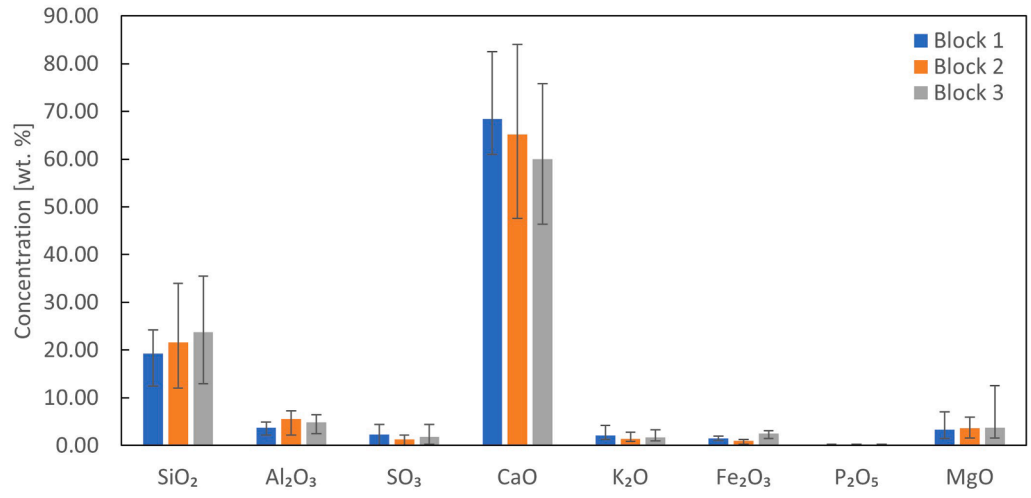

Fig. 9. Average chemical composition of the surface layer of the three concrete blocks containing different cement types.

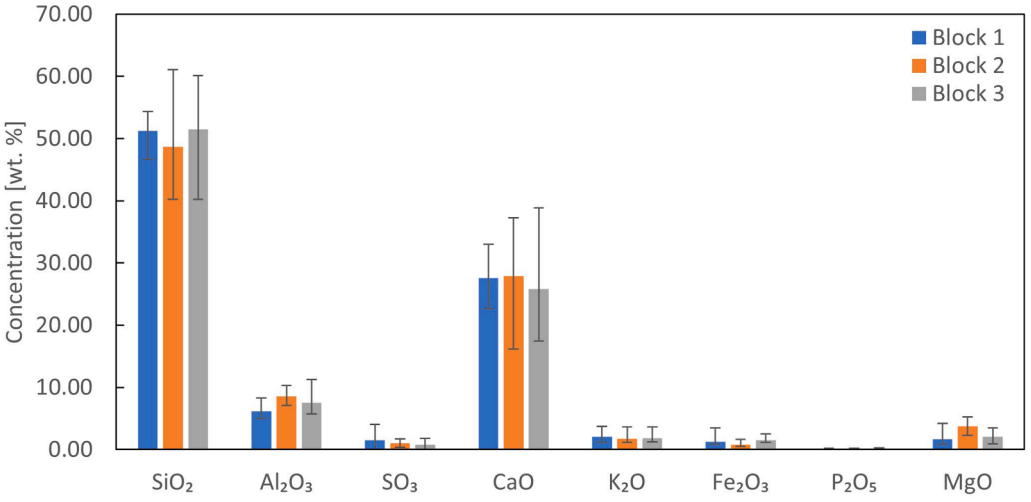

Fig. 10. Average chemical composition of the mortar layer of the three concrete blocks.

respectively. This would substantially increase processing efficiency in practice when large numbers of samples need to be processed within a given time period. From theory, it is known that elements with atomic numbers below 16 present significant measurement challenges using HXRF due to their lower energy emissions [6,39]. Magnesium (Mg), with atomic number 12, exemplifies this limitation, resulting in reduced detection reliability. This particularly explains the observed fluctuations in the reliability observed in this study (see Supplementary Table S1). While these deviations suggest that MgO may therefore not be ideal as an oxide for cement identification, materials containing higher MgO concentrations can still be effectively distinguished from those with lower MgO content based on relative composition analysis. From a practical applicability standpoint, powder measurement times can therefore be reduced from 50 s to 5 s, as all powders demonstrate reliability above 85 % for a 5-second measurement duration. However, practical considerations recommend against durations below 10 s, as the HXRF device typically requires 5–10 s stabilization before displaying initial results. Therefore, 10 s represents a recommended lower boundary for powder measurements in field applications.

The analysis of measurement time requirements for concrete blocks provides key insights into the reliability of HXRF characterization across sample types. Compared to powders, concrete blocks generally require longer measurement durations to achieve comparable reliability, which aligns with theoretical expectations due to matrix effects. X-rays penetrate more effectively in fine powders, whereas larger particles reduce penetration depth, yielding responses primarily from surface or larger grains. Additionally, heterogeneity and mineralogical differences further influence measurement accuracy [15]. Most concrete block samples achieved the 95 % reliability threshold at measurement times of 80 s or longer, with block 3.5 being an exception, requiring 190 s to reach this standard. This variation highlights the influence of compositional heterogeneity on measurement reliability in solid concrete samples. At reduced measurement times, however, most blocks maintained reliability above 85 %, with blocks 2.5 and 3.5 requiring minimum measurement durations of 20 s to achieve this level of confidence. Based on these findings, a minimum 20-second measurement time is recommended for field applications involving solid concrete. Results from this study (listed in Supplementary Figures S1-S3 and Supplementary Tables S2-S4) confirm measurement stability when measurement time is decreased from 300 to 20 s, suggesting that shorter measurement times are sufficient for field applications. However, measurement times below 20 s showed significant variations, indicating that this measurement duration represents a practical lower threshold for reliable concrete product analysis. Consistent with the powder analysis findings, magnesium exhibited the largest measurement deviations across all timeframes, confirming the challenges associated with detecting lighter

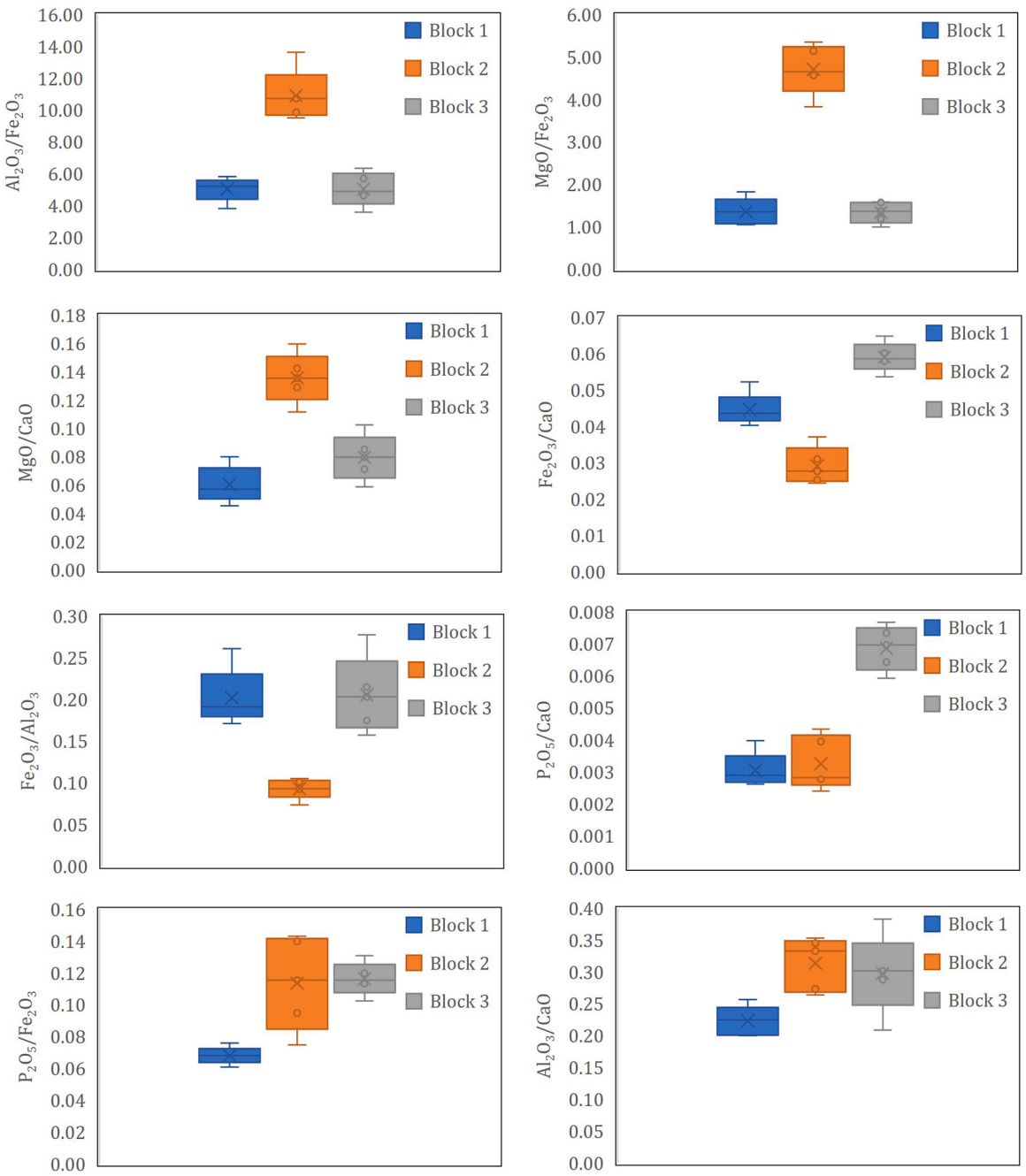

Fig. 11. Normalized ratio's of interest for the determination of the cement types in the blocks. After block 2 (CEM III/B-based) has been identified, a clear distinction can be made between block 1 (CEM I-based) and 3 (CEM II/B-V-based).

Table 5
Normalized range of the ratio between certain oxides and CaO, Al_2O_3 or Fe_2O_3 that result in an identification of the cement type within the concrete blocks. Block 1 is CEM I based concrete, block 2 is CEM III/B based concrete and block 3 is CEM II/B-V based concrete.

		Block 1	Block 2	Block 3
Oxide	Al_2O_3	0.2 – 0.26	0.26 – 0.35	0.21 – 0.38
/	Fe_2O_3	0.04 – 0.05	0.02 – 0.04	5.37 – 6.49
CaO	P_2O_5	0.003 – 0.004	0.002 – 0.004	0.006 – 0.008
	MgO	0.05 – 0.08	0.11 – 0.16	0.06 – 0.10
Oxide/Al_2O_3	Fe_2O_3	0.17 – 0.26	0.07 – 0.11	0.16 – 0.28
Oxide	Al_2O_3	3.84 – 5.84	9.51 – 13.64	3.60 – 6.36
/	P_2O_5	0.06 – 0.08	0.07 – 0.14	0.10 – 0.13
Fe_2O_3	MgO	1.05 – 1.82	3.83 – 5.35	1.01 – 1.59

elements using HXRF technology.

4.2. Moisture influence and efflorescence effect

The influence of moisture on the HXRF measurement results is an important factor to consider, particularly for concrete exposed to outdoor conditions. Nedelkjović et al. [28] found that moisture significantly impacts measured oxide concentrations, except for Fe_2O_3. Similar trends were observed in this study: with increasing moisture content, CaO levels increased while SiO_2 and Al_2O_3 decreased. In contrast, SO_3 and MgO remained detectable. However, the specific changes varied depending on the cement type. While moisture influenced oxide concentrations, these changes were not significant enough to prevent cement type identification, as oxide concentrations between cement

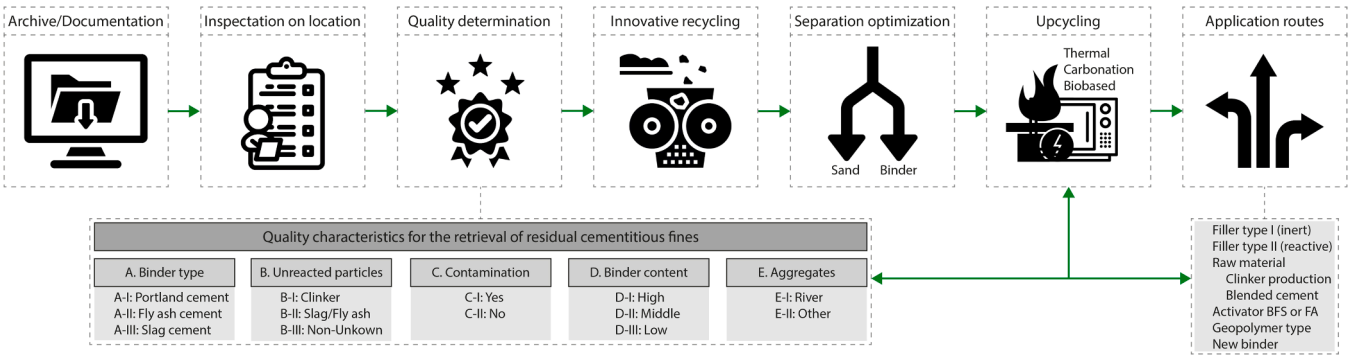

Fig. 12. Process steps for retrieval of high-quality residual cementitious fines. It is important to gain insight into the concrete's chemical composition with respect to the present cement type prior to demolition and crushing for determination of the potentially most suitable upcycling approach and application potential of retrieved fines.

types remained distinctly different. CEM III/B prisms showed only minor concentration changes. CEM I appeared more sensitive to moisture, with noticeable variations in SiO_2, Al_2O_3, CaO, K_2O, and SO_3 concentrations, while Fe_2O_3 and MgO remained largely stable. For CEM II/B-V prisms, concentration changes became more apparent with increased moisture. Despite these moisture-induced variations, all measurements remained within the acceptable range (>85 % reliability threshold) for accurate cement type identification. Other factors, such as efflorescence or surface coatings, appear to have a more pronounced influence on cement identification.

Analysis of the chemical composition as measured by HXRF relative to block position (see results shown in Supplementary Figures S4-S6) revealed significant variability, largely influenced by surface conditions. In some locations, the absence of a cement layer indicated that measurements were taken directly from the mortar, leading to inconsistencies. Another notable factor affecting surface composition was the efflorescence effect, characterized by elevated calcium concentrations in the outer layer. This resulted in an overestimation of CaO content, consistent with findings by Nedeljković et al. [28], who reported this phenomenon as particularly pronounced in CEM I cements due to their higher intrinsic CaO levels. However, in this study, the extent of efflorescence could not be linked to the cement type. The highest CaO concentration (84.1 %) was measured on Block 2.5 (see Supplementary Figures S4-S6 for results), which could lead to misclassification as a CEM I cement instead of the actual CEM III/B. Conversely, some measurements showed significantly lower calcium values (e.g., 47.6 % for Block 2), likely due to weathering resulting in eroded surface layers. These fluctuations in CaO also affect the relative concentrations of other elements critical for cement identification. In indoor environments, the surface layer may provide a reliable indication of the cement type. However, paints or coatings commonly applied indoors can obstruct access to the original cement surface and should be removed before HXRF analysis. Furthermore, the age of the concrete plays a role in surface composition, particularly in outdoor conditions. EoL concrete structures are typically much older than the blocks used in this study, which may lead to even greater surface degradation over time and subsequently loss of the surface layer.

4.3. Removal of the surface layer

Given the challenges with the surface layer mentioned above, the effect of removing the surface layer of aged concrete objects on HXRF analysis results was analysed in this study. Nedeljković et al. [28] recommend ultrafine sandpaper (P-grade 2000 or grit size <10 μm) to remove calcium carbonate layers and expose underlying cement paste. However, in this study, this approach was found to be impractical for outdoor concrete elements. The sandpaper lacked sufficient durability across variable surface morphologies, and operator technique significantly influenced removal thickness. Since HXRF technology will be deployed across multiple companies and operators, measurement approaches with minimal operator dependency are strongly preferred.

Consequently, the investigation was expanded to deeper concrete layers (0.1 – 5 mm), where aggregate presence introduces new variables requiring consideration. During testing, the HXRF device was positioned between visible aggregates when possible. The siliceous origin of aggregates in the investigated concrete blocks resulted in predictably elevated SiO_2 concentrations in these layers. Despite this, specific oxide concentrations and distinctive elemental combinations were identified that effectively determine the cement type following removal of the surface layer.

For block 1 (CEM I-based), cement identification relied primarily on lower Al_2O_3 content paired with higher Fe_2O_3 concentrations. The differentiation between blocks 2 (CEM III/B-based) and 3 (CEM II/B-V-based) was achieved by the higher MgO and lower Fe_2O_3 concentrations of block 2. Notably, SiO_2 was an unreliable identification marker due to significant aggregate influence on its concentrations. Element ratios emerged as particularly valuable for identification, providing clearer insights than absolute concentrations. These ratios, presented in Table 5 and Fig. 11, demonstrate that ratios between CaO, Al_2O_3, Fe_2O_3, P_2O_5, and MgO can effectively be used to identify concrete cement type across various samples. The table also establishes preliminary threshold ranges facilitating accurate cement identification under field conditions. Therefore, when measurements can be performed on cement stone between visible aggregates, HXRF technology demonstrates significant potential for accurate cement identification even in deeper concrete layers, which represents an important advancement for practical field applications in concrete recycling and assessment.

5. Conclusion

This study investigated a practical measurement approach using handheld X-Ray Fluorescence (HXRF) to identify present cement types in End-of-Life (EoL) concrete. The following key conclusions can be drawn:

- Measurement time and sample type:
  For the investigated cementitious powders, a 50-second measurement time achieves 95 % reliability, although shorter durations (down to 10 s) are acceptable in practice as lower reliability thresholds still enable cement identification. For concrete blocks, 80 s ensures 95 % reliability, with 20 s being a practical minimum. Surface layer measurements require approximately 30 measurement points for reliable cement identification. However, accuracy is compromised by efflorescence, coatings, weathering and inconsistent surface removal, making deeper-layer analysis preferable in such cases.

- Moisture and Efflorescence effects:
  Moisture has a negligible impact on cement type identification, with variations remaining within acceptable bounds for reliable classification. In contrast, efflorescence can significantly distort oxide concentrations and must be accounted for or removed.
- Oxide markers for cement identification:
  After surface removal, cement types can be reliably distinguished based on oxide concentrations and elemental ratios. Key differentiators include Al_2O_3, Fe_2O_3, P_2O_5, and MgO levels.
  - o CEM I is characterized by lower Al_2O_3 (average 6.2 %) concentrations.
  - o CEM II/B-V and CEM III/B are differentiated by MgO (average 2.1 % versus 3.7 %), Fe_2O_3 (average 1.5 % versus 0.8 %), and P_2O_5 (average 0.18 % versus 0.09 %) levels.
  - o Specific ratios support classification:
    - CEM III/B: $Al_2O_3/Fe_2O_3 > 9.0$, $MgO/Fe_2O_3 > 3.0$, $MgO/CaO > 0.11$, $Fe_2O_3/Al_2O_3 < 0.11$ and $Fe_2O_3/CaO < 0.04$.
    - CEM II/B-V: $P_2O_5/CaO > 0.005$ and $P_2O_5/Fe_2O_3 > 0.1$.
    - CEM I generally shows opposite trends: $P_2O_5/CaO < 0.005$ and $P_2O_5/Fe_2O_3 < 0.1$.

Several recommendations emerge from this research along with suggestions for future work. For reliable field application, the surface layer should be removed to avoid errors due to coatings or weathering. Future studies should aim to refine oxide thresholds and broaden classification across more cement types. The authors foresee huge potential for integrating machine learning techniques using HXRF-derived chemical composition data to enhance the precision and scalability of cement identification in diverse concrete compositions. However, this approach remains speculative and would require systematic validation and research to address potential challenges.

Declaration of Competing Interest

The authors declare that they have no known competing financial interests or personal relationships that could have appeared to influence the work reported in this paper.

Acknowledgements

The authors like to thank Urban Mine B.V. for funding this research.

Appendix A. – Chemical composition reproducibility of the CEM I based concrete blocks with and without surface removal for 3 measurement locations (A, B, C; 3 repeated measurements per location)

Reproducibility tests revealed good precision for most oxides critical to cement classification (Table A.1-A.2). Coefficient of variation values were consistently low. While MgO showed higher variability, precision was improved after surface removal. Most oxides show reduced standard deviations and CV values (Tables A.1 versus A.2) after surface removal. This suggests that surface contamination or weathering can affect measurement reproducibility. Surface removal improved measurement precision, reinforcing the importance of including this in the methodology. Even with the higher variability observed for MgO, the precision achieved is sufficient for distinguishing between different cement types.

A.1
Surface layer measurements Block 1 (Std Dev: standard deviation, CV: coefficient of variance)

		SiO_2	Al_2O_3	SO_3	CaO	K_2O	Fe_2O_3	MgO
Location A	1 [wt%]	18.385	3.708	3.467	70.694	1.664	1.775	0.701
	2 [wt%]	18.283	3.785	3.533	70.355	1.673	1.833	0.895
	3 [wt%]	18.335	3.978	3.480	68.172	1.597	1.737	3.669
	Average [wt%]	18.334	3.824	3.493	69.740	1.645	1.782	1.755
	Std Dev [wt%]	0.051	0.139	0.035	1.369	0.041	0.048	1.660
	CV [%]	0.28	3.65	0.99	1.96	2.52	2.71	94.61
Location B	1 [wt%]	22.760	4.049	3.500	62.292	1.237	1.490	4.731
	2 [wt%]	22.806	4.079	3.653	62.431	1.222	1.573	4.126
	3 [wt%]	22.669	3.819	3.760	64.510	1.258	1.573	1.830
	Average [wt%]	22.745	3.982	3.638	63.078	1.239	1.546	3.562
	Std Dev [wt%]	0.070	0.142	0.131	1.242	0.018	0.048	1.530
	CV [%]	0.31	3.57	3.60	1.97	1.44	3.10	42.96
Location C	1 [wt%]	20.899	4.494	2.597	65.426	1.739	1.599	3.488
	2 [wt%]	20.908	4.404	2.681	66.312	1.787	1.590	2.433
	3 [wt%]	20.352	4.426	2.626	67.874	1.811	1.697	1.260
	Average [wt%]	20.720	4.441	2.635	66.537	1.779	1.629	2.394
	Std Dev [wt%]	0.318	0.047	0.043	1.239	0.037	0.060	1.114
	CV [%]	1.54	1.05	1.61	1.86	2.06	3.67	46.55

A.2
Measurements after surface removal of Block 1 (Std Dev: standard deviation, CV: coefficient of variance)

		SiO_2	Al_2O_3	SO_3	CaO	K_2O	Fe_2O_3	MgO
Location A	1 [wt%]	52.350	5.993	2.286	26.723	1.579	0.948	1.532
	2 [wt%]	52.383	5.899	2.182	27.003	1.600	1.044	0.973
	3 [wt%]	52.250	5.639	2.232	27.146	1.621	1.018	1.366
	Average [wt%]	52.328	5.844	2.233	26.957	1.600	1.003	1.290
	Std Dev [wt%]	0.069	0.183	0.052	0.215	0.021	0.050	0.287
	CV [%]	0.13	3.14	2.34	0.80	1.33	4.97	22.27
Location B	1 [wt%]	50.904	5.096	2.061	28.774	1.145	1.151	2.554
	2 [wt%]	51.350	5.564	1.990	27.161	1.173	1.341	2.881
	3 [wt%]	51.591	5.521	1.940	27.063	1.198	1.383	2.594
	Average [wt%]	51.281	5.394	1.997	27.666	1.172	1.292	2.676

(*continued on next page*)

A.2 (*continued*)

		SiO_2	Al_2O_3	SO_3	CaO	K_2O	Fe_2O_3	MgO
	Std Dev [wt%]	0.348	0.258	0.061	0.961	0.027	0.124	0.178
	CV [%]	0.68	4.79	3.06	3.47	2.27	9.61	6.67
Location C	1 [wt%]	52.504	5.276	1.287	28.054	1.613	0.948	1.579
	2 [wt%]	53.063	5.169	1.272	27.738	1.577	0.924	1.350
	3 [wt%]	52.817	5.132	1.334	27.854	1.605	0.892	1.586
	Average [wt%]	52.795	5.193	1.298	27.882	1.598	0.921	1.505
	Std Dev [wt%]	0.280	0.075	0.033	0.160	0.019	0.028	0.134
	CV [%]	0.53	1.44	2.52	0.57	1.18	3.04	8.94

Appendix B. – Cross validation of HXRF and desktop XRF results

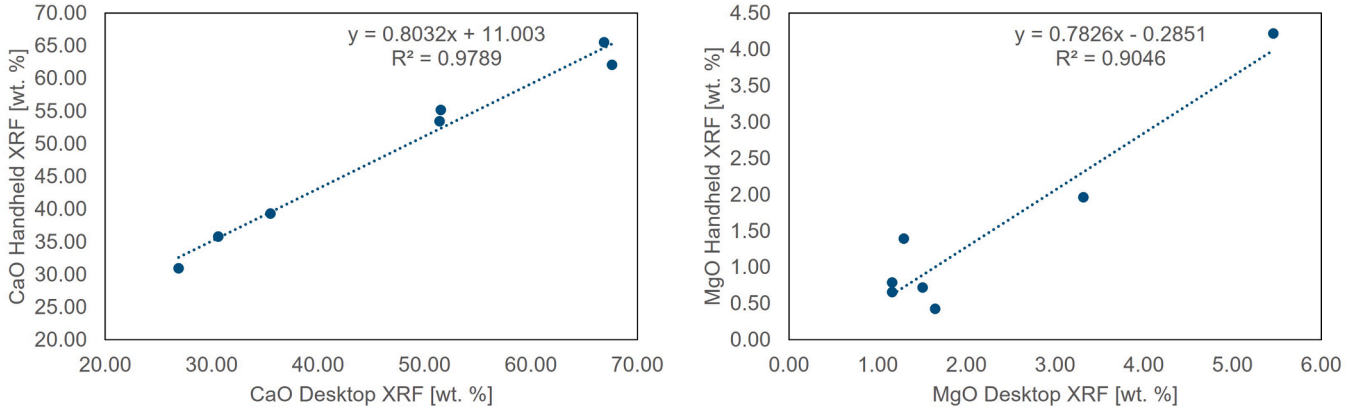

B.1. Cross validation of HXRF and desktop XRF results of CaO and MgO

B.2
Overview of R^2-values of the cross validation of HXRF and desktop XRF for various oxides

	SiO_2	Al_2O_3	SO_3	CaO	Fe_2O_3	MgO
R^2	0.9866	0.9266	0.9493	0.9789	0.9287	0.9046

Appendix C. Supporting information

Supplementary data associated with this article can be found in the online version at doi:10.1016/j.conbuildmat.2025.144293.

Data availability

Data will be made available on request.

References

[1] A. Alberda van Ekenstein, H. Jonkers, M. Ottelé, Downstream processing of End-of-Life concrete for the recovery of high-quality cementitious fractions, Cement (2024) 100121, https://doi.org/10.1016/j.cement.2024.100121.
[2] E. Benhelal, G. Zahedi, E. Shamsaei, A. Bahadori, Global strategies and potentials to curb CO2 emissions in cement industry, J. Clean. Prod. 51 (2013) 142–161, https://doi.org/10.1016/j.jclepro.2012.10.049.
[3] L. Bertolini, F. Lollini, Effects of weathering on colour of concrete paving blocks, Eur. J. Environ. Civ. Eng. 15 (6) (2011) 939–957.
[4] O. Burgos-Montes, M. Palacios, P. Rivilla, F. Puertas, Compatibility between superplasticizer admixtures and cements with mineral additions, Constr. Build. Mater. 31 (2012) 300–309.
[5] Z. Chen, W.M. Gibson, H. Huang, High definition X-ray fluorescence: principles and techniques, Xray Opt. Instrum. 2008 (2008), https://doi.org/10.1155/2008/318171.
[6] Y. Declercq, N. Delbecque, J. De Grave, P. De Smedt, P. Finke, A.M. Mouazen, A. Verdoodt, A comprehensive study of three different portable XRF scanners to assess the soil geochemistry of an extensive sample dataset, Remote Sens. 11 (21) (2019) 2490.
[7] A. Di Maria, J. Eyckmans, K. Van Acker, Downcycling versus recycling of construction and demolition waste: Combining LCA and LCC to support sustainable policy making, Waste Manag. 75 (2018) 3–21, https://doi.org/10.1016/j.wasman.2018.01.028.
[8] A. Di Maria, J. Eyckmans, K. Van Acker, Use of LCA and LCC to help decision-making between downcycling versus recycling of construction and demolition waste, Adv. Constr. Demolition Waste Recycl. (2020) 537–558, https://doi.org/10.1016/B978-0-12-819055-5.00026-7.
[9] C. Dow, F.P. Glasser, Calcium carbonate efflorescence on Portland cement and building materials, Cem. Concr. Res. 33 (1) (2003) 147–154.
[10] L. Ge, W. Lai, Y. Lin, Influence of and correction for moisture in rocks, soils and sediments on in situ XRF analysis, X-Ray Spectrom. Int. J. 34 (1) (2005) 28–34.
[11] P.C. Hewlett. Lea's Chemistry of Cement and Concrete, 4 ed., Butterworth-Heinemann, UK, 2004.
[12] Hitachi High-Tech Analytical Science. (2019). XMET8000 Series Supervisor Guide. (6.0).
[13] Hitachi High-Tech Analytical Science. (2021). X-MET8000 Expert Geo Calibration datasheet. Retrieved from.
[14] J. Hu, T. Cavalline, M. Mamirov, A. Dey, 2022, ACI CRC 2019 P0027: Effective Characterization of Recycled Concrete Aggregate (RCA) for Concrete Applications..
[15] A.M. Hunt, R.J. Speakman, Portable XRF analysis of archaeological sediments and ceramics, J. Archaeol. Sci. 53 (2015) 626–638.

[16] Koninklijk Nederlands Meteorologisch Instituut. (2022). Jaar 2022 - Extreem warm, recordzonnig en droog. Retrieved from ⟨https://www.knmi.nl/nederland-nu/klimatologie/maand-en-seizoensoverzichten/2022/jaar⟩.
[17] Koninklijk Nederlands Meteorologisch Instituut. (2023). Jaar 2023 - Recordwarm, recordnat en zeer zonnig. Retrieved from ⟨https://www.knmi.nl/nederland-nu/klimatologie/maand-en-seizoensoverzichten/2023/jaar⟩.
[18] P. Kreijger, The skin of concrete composition and properties, Mat. ériaux Et. Constr. 17 (1984) 275–283.
[19] V. Laperche, B. Lemière, Possible pitfalls in the analysis of minerals and loose materials by portable xrf, and how to overcome them, Minerals 11 (1) (2020) 33.
[20] I. Liritzis, N. Zacharias, Portable XRF of archaeological artifacts: current research, potentials and limitations, Xray Fluoresc. Spectrom. (XRF) Geoarchaeol. (2011) 109–142.
[21] M.A. Longhi, Z. Zhang, E.D. Rodríguez, A.P. Kirchheim, H. Wang, Efflorescence of alkali-activated cements (geopolymers) and the impacts on material structures: a critical analysis, Front. Mater. 6 (2019) 89.
[22] Y. Luo, X. Gao, D. Wang, Y. Liu, Q. Zhang, J. Li, G. Xue, Study on the efflorescence behavior of concrete by adding metakaolin, J. Build. Eng. 83 (2024) 108396.
[23] C. Ma, H. Dou, Z. Zhao, X. Qiu, H. Li, X. Wang, Review of in-situ non-and micro-destructive techniques for pigment analysis in architectural heritage, npj Herit. Sci. 13 (1) (2025) 222.
[24] H. Mehdizadeh, X. Cheng, K.H. Mo, T.-C. Ling, Upcycling of waste hydrated cement paste containing high-volume supplementary cementitious materials via CO2 pre-treatment, J. Build. Eng. 52 (2022) 104396, https://doi.org/10.1016/j.jobe.2022.104396.
[25] K.K. Mensah, Reliability assessment of structural concrete with special reference to shear resistance, Stellenbosch Stellenbosch Univ. (2012).
[26] S.A. Miller, F.C. Moore, Climate and health damages from global concrete production, Nat. Clim. Change (2020) 1–5, https://doi.org/10.1038/s41558-020-0733-0.
[27] D.C. Montgomery, G.C. RungerApplied statistics and probability for engineers2010, John wiley & sons.
[28] M. Nedeljković, N. Tošić, P. Holthuizen, F. França de Mendonça Filho, O. Çopuroğlu, E. Schlangen, S. Fennis, Non-destructive screening methodology based on handheld XRF for the classification of concrete: cement type-driven separation, Mater. Struct. 56 (3) (2023) 54, https://doi.org/10.1617/s11527-023-02147-3.
[29] M. Nedeljković, J. Visser, T.G. Nijland, S. Valcke, E. Schlangen, Physical, chemical and mineralogical characterization of Dutch fine recycled concrete aggregates: a comparative study, Constr. Build. Mater. 270 (2021) 121475, https://doi.org/10.1016/j.conbuildmat.2020.121475.
[30] Nederlands Normalisatie-instituut. (2016). NEN-EN 196-1 Methods of testing cement - Part 1: Determination of strength. Belgium: CEN Brussels.
[31] H.Y. Qasrawi, Concrete strength by combined nondestructive methods simply and reliably predicted, Cem. Concr. Res. 30 (5) (2000) 739–746.
[32] Ł. Sadowski, D. Stefaniuk, The effect of surface treatment on the microstructure of the skin of concrete, Appl. Surf. Sci. 427 (2018) 934–941.
[33] A.R. Schneider, B. Cancès, C. Breton, M. Ponthieu, X. Morvan, A. Conreux, B. Marin, Comparison of field portable XRF and aqua regia/ICPAES soil analysis and evaluation of soil moisture influence on FPXRF results, J. Soils Sediment. 16 (2016) 438–448.
[34] I. Soroka, Portland cement paste and concrete, Macmillan International Higher Education, 1979.
[35] P. Taylor, E. Yurdakul, H. Ceylan, 2012, Concrete pavement mixture design and analysis (MDA): Application of a portable x-ray fluorescence technique to assess concrete mix proportions.
[36] P. Tesinova, 2011, Advances in composite materials: analysis of natural and man-made materials: BoD–books on demand.
[37] G. Van der Wegen, Een overzicht van innovatieve recyclingsmethoden, Betoniek (2020) *2020–2021*.
[38] M. Verweij, Terugwinnen van cement uit beton, Betoniek 2020 3 (2020).
[39] K.E. Young, C.A. Evans, K.V. Hodges, J.E. Bleacher, T.G. Graff, A review of the handheld X-ray fluorescence spectrometer as a tool for field geologic investigations on Earth and in planetary surface exploration, Appl. Geochem. 72 (2016) 77–87.
[40] M. Zajac, J. Skibsted, P. Durdzinski, F. Bullerjahn, J. Skocek, M.B. Haha, Kinetics of enforced carbonation of cement paste, Cem. Concr. Res. 131 (2020) 106013, https://doi.org/10.1016/j.cemconres.2020.106013.
[41] S. Zhang, Z. Ghouleh, Y. Shao, Effect of carbonation curing on efflorescence formation in concrete paver blocks, J. Mater. Civ. Eng. 32 (6) (2020) 04020127.